Development of Soil Moisture Drought Index to Characterize Droughts

Mohammad M. Sohrabi[1]; Jae H. Ryu, M.ASCE[2]; John Abatzoglou[3]; and John Tracy[4]

Abstract: A new drought index termed the "soil moisture drought index (SODI)" is developed to characterize droughts. The premise of the index is based on how much water is required to attain soil moisture at field capacity. SODI captures variations of precipitation, temperature, and soil moisture over time. Three widely used drought indices, including the standardized precipitation index (SPI), the standardized precipitation evapotranspiration index (SPEI), and the self-calibrated palmer drought index (sc-PDSI) are compared with SODI along with local hydrological variables such as streamflow, reservoir storage, and groundwater level for cross-validation. The result indicates that SODI reacts more evidently to relate changes in precipitation and temperature than SPI and SPEI by characterizing soil moisture over time. Results also show that SODI outperforms the existing drought indices in the sense that SODI can detect and quantify the extended severe droughts associated with climate variability and change. SODI will add momentum to build a case toward the use of soil moisture information for drought analysis in a changing environment. **DOI: 10.1061/(ASCE)HE.1943-5584.0001213.** © *2015 American Society of Civil Engineers.*

Author keywords: Drought; Drought index; Hydrological drought; Soil moisture drought index (SODI).

Introduction

Droughts bring profound hydrological, ecological, agricultural and economic impacts. Recent droughts in the United States (US) have resulted in the enactment of emergency drought plans to mitigate dwindling water supplies in the Colorado River basin and crop failure in many southeastern states (Manuel 2008). The historic drought in the state of Texas in 2011, in particular, had significant economic impacts on agricultural sectors and other food business, with nearly $7 billion in economic losses reported by Texas A&M University's AgriLife Extension Office (Ryu et al. 2014). Although economic losses linked to drought are prevalent across the country (Mishra and Singh 2010), drought mitigation exercises are still challenging due to a unique characteristic of drought. Because of its slow onset and typically wide spatial domain, it is difficult to define the beginning or end of a drought (Dracup et al. 1980; Ryu et al. 2004; Wilhite and Glantz 1985; Yevdjevich 1967).

Drought produces a complex sequence of intertwined impacts, ranging from direct impacts to concerns over long-term water sustainability (Ryu et al. 2014). Yet, understanding historical droughts and their impacts is important for drought assessments, planning, and management of water resources (Mishra and Singh 2010). A drought index simplifies the complex characteristics of drought by assimilating raw data, such as precipitation and temperature, to describe drought properties, which are readily applicable for drought analysis (Mishra and Singh 2010; Zargar et al. 2011). Drought indices can identify onset and termination of droughts and quantify drought severity. Therefore, drought indices are useful tools to mitigate drought impacts by defining thresholds and alarm levels (Niemeyer 2008), early warnings (Kogan 2000), drought risk analysis (Hayes et al. 2004), and ultimately, they can be used for long-term drought planning and decision making.

More than 100 drought indices have been developed to address and quantify the intertwined nature of drought (Niemeyer 2008). Some drought indices can merely reflect one type of drought impact, which limits their scope of application. For instance, the crop moisture index (CMI) (Palmer 1968) or surface water supply index (SWSI) (Dezman et al. 1982) can be deployed to detect agricultural drought or hydrological drought, respectively. A limited number of indices, such as the standardized precipitation index (SPI) (McKee et al. 1993) and the standardized precipitation evapotranspiration index (SPEI) (Vincente-Serrano et al. 2010), respond to different types of drought, including meteorological, agricultural, and hydrological droughts. Among all drought indices, the Palmer drought severity index (PDSI) (Palmer 1965), SPI, and SPEI have been well-tested and widely used due to their good performance and capability to describe drought at regional and national levels (Mishra and Singh 2010; Zargar et al. 2011).

PDSI defined as a function of precipitation, temperature, and the available water content of the soil (soil water balance). PDSI's applicability and versatility was often criticized due to its drawbacks (Alley 1984; Guttman et al. 1992; Karl 1983; Wells et al. 2004). Poor performances of PDSI in the western US where complex terrain and landscape is prevalent led to the revised PDSI known as self-calibrated Palmer drought severity index (sc-PDSI) (Wells et al. 2004). Unlike PDSI, the sc-PDSI accounts for the expected variability of weather conditions between locations so that the climatic characteristic and the associated factor can be adjusted automatically based on local information. After sc-PDSI, however, the other deficiencies of the index are still discussed. For example, abrupt changes in PDSI value from one month to the next, are not realistic (Alley 1984). As Alley pointed out, in many cases, a dry month (e.g., PDSI ≤ -2) is immediately followed by a wet month

[1]Ph.D. Student, Dept. of Biological and Agricultural Engineering, Univ. of Idaho, Boise, ID 83702.

[2]Assistant Professor, Dept. of Biological and Agricultural Engineering, Univ. of Idaho, 322 E. Front St., Boise, ID 83702 (corresponding author). E-mail: jryu@uidaho.edu

[3]Assistant Professor, Dept. of Geography, Univ. of Idaho, Moscow, ID 83844.

[4]Director, Idaho Water Resources Research Institute, Univ. of Idaho, Boise, ID 83702.

Note. This manuscript was submitted on August 27, 2014; approved on February 18, 2015; published online on March 23, 2015. Discussion period open until August 23, 2015; separate discussions must be submitted for individual papers. This paper is part of the ***Journal of Hydrologic Engineering***, © ASCE, ISSN 1084-0699/04015025(15)/$25.00.

(e.g., PDSI $\geq$ 1), But, this is not likely to happen in reality. He also indicated that the probability of ending a dry/wet spell (Pe) was not well defined in PDSI. Dai (2011), Van der Schrier et al. (2011), and Paulo et al. (2012) reported non-Gaussian histogram of PDSI/sc-PDSI at many locations. They showed the low frequency of PDSI/sc-PDSI at near normal category ($-0.5 \leq$ sc-PDSI ≤ 0.5) at many locations.

The SPI is also widely used to define drought, but merely based on precipitation variation. Nonetheless, SPI has been applied broadly due to its simple concept and computational ease of use. Mishra and Singh (2010) and Paulo et al. (2012) illustrated that the SPI values are significantly affected by the length of precipitation record and choice of probability distribution.

Unlike SPI, the SPEI captures changes in temperature-induced evapotranspiration (Vincente-Serrano et al. 2010; Mishra and Singh 2010; Zargar et al. 2011; Paulo et al. 2012). SPEI is based on difference between precipitation (supply) and evapotranspiration (demand), which is referred to a climatic water balance. The choice of probability distribution can determine SPEI values. In addition, SPEI is incapable of considering water stored in soil, which is an important factor, particularly at semi-arid and arid areas (Vaezi 2013). Paulo et al. (2012) reported that PDSI better identifies the supply-demand dynamics than SPEI and SPI, because PDSI is developed based on soil water balance so it considers actual evapotranspiration rather than potential evapotranspiration. They claimed that PDSI responds more evidently to precipitation anomalies due to considering soil water retention.

Although these drought indices (PDSI, SPI, and SPEI) are typically used for drought analysis, they share a common feature, namely a time independency. Thus, they are developed for a targeted month (e.g., January, February, etc.) that does not necessarily maintain the continuity during month-to-month transitions. As such, the main purpose of this study is to develop a new drought index termed the "soil moisture drought index (SODI)," which combines advantages of the aforementioned drought indices by characterizing soil water retention processes determining dry/wet condition in subsequent time steps. In other words, a time-dependent drought index is critical to represent soil moisture departure within a soil column at a current time step contributing additional moisture for hydrologic processes in the following time step.

This paper is organized as follows. Methodology for SODI is first described and followed by the study area and data. Next, SODI's characteristics are discussed in the result section by comparing them with other drought indices along with hydrological variables, including streamflow, reservoir, and groundwater for cross-validation. The climate-induced SODI is another avenue to verify how SODI can be used for potential drought outlooks driven by uncertain future climate. Finally, a summary and conclusion are discussed.

Methodology

Soil Moisture Drought Index (SODI)

The SODI incorporates multiple environmental variables, including temperature, precipitation, potential evapotranspiration (PE), runoff, and soil moisture. A basic premise of the computational process is derived from the two-layer "bucket" model of the soil column defined by Palmer (1965) [Eqs. (8)–(15) in "Appendix"]. Available water capacity (AWC)—the amount of soil moisture between the field capacity (FC) and the permanent wilting point (WP) for a soil layer (Hillel 1982; Veihmeyer and Hendrickson 1927)—is first characterized because AWC is a proper surrogate for soil

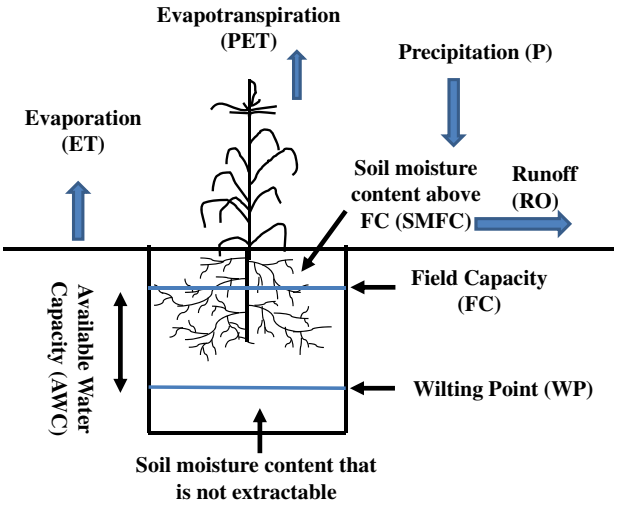

Fig. 1. Conceptual diagram of moisture supply and demand in soil column

column associated with soil texture, porosity, bulk density, and osmatic pressure (Vaezi 2013) (Fig. 1). In this study, 25.4 mm (1 in.) of AWC was assigned for potentially available water for plants at the first layer (Palmer 1965), while AWC of the second layer depends on soil characteristics of the region.

For potential evapotranspiration (PE), Thornthwaite's method (Thornthwaite 1948) was used because it has been broadly discussed and adapted by many previous studies (Dai 2011; Van der Schrier et al. 2011; Vicente-Serrano et al. 2010). A key parameter, the moisture departure at a month i (D_i), however, has been revised to better represent soil moisture contributions to local droughts.

Unlike moisture departure (D) in PDSI and SPEI, moisture departure in SODI accounts for climate memory, which is enraptured in soil moisture conditions at the current month affected by the previous month. For a water budget analysis, runoff (RO), representing overland flow and soil water content above field capacity (SMFC in Fig. 1), contributes additional moisture for hydrologic conditions in the following time step. Therefore, potential evapotranspiration (PE) plus soil moisture deficiency (SMD) can indicates how much moisture is required to keep up soil water content at the field capacity level based on current and previous moisture conditions in the field. In mathematical terms, D_i can be defined as

$$D_i = (P_i + L_i + \mathrm{RO}_{i-1}) - (\mathrm{PE}_i + \mathrm{SMD}_{i-1}) \quad (1)$$

where P_i = total amount of precipitation at the current month, i; L_i = moisture loss from soil column at the current month; RO_{i-1} = surface runoff at the previous month and stored in SMFC; PE_i = potential evapotranspiration at the current month, i; and SMD_{i-1} = soil moisture deficiency at the previous month as defined by

$$\mathrm{SMD}_{i-1} = \mathrm{AWC} - \mathrm{SM}_{i-1} \quad (2)$$

where AWC = available water capacity of the soil layers; and SM_{i-1} = soil moisture content of the previous month.

Basically, the first and second parenthesis in Eq. (1) indicates moisture supply and demand for each time step, respectively. Fig. 1 illustrates a conceptual diagram of soil moisture supply and demand in the soil column. The supply moisture term accounts for all available moisture, while the moisture demand term indicates the demanded water needed to keep up soil moisture content at

FC. Therefore, D_i determines moisture departure from the FC. For example, if precipitation is larger than evapotranspiration in a month, no moisture loss from soil (L_i) occurs so that evaporation (ET) is equal to potential evapotranspiration (PET). In other words, if the previous month was a wet month ($D_{i-1} > 0$), then RO_{i-1} is greater than zero and SMD_{i-1} is zero so that D_i becomes positive. Consequently, D_i can be positive or negative depending upon how much of the moisture deficiency in the previous month (SMD_{i-1}) was compensated by available moisture at the current month.

For another example, if available moisture for evapotranspiration is limited in a month ($P_i < \mathrm{PE}_i$), then moisture loss from the soil column is inevitable. Thus, if the previous month was a dry month, then RO_{i-1} is zero and SMD_{i-1} is greater than zero so that D_i becomes negative. Since both SMD_{i-1} and RO_{i-1} in Eq. (1) incorporate the previous time step's condition into moisture departure (D_i), SODI can be a continuous index.

To apply SODI for multiple time scales, moisture departure, D_i, at starting time i, is aggregated to create a new time series denoted as $D^*_{i,k}$ for the selected time window (k). For example, for a 3-month window ($k = 3$), aggregated moisture departure (D^*) at month, i, starting for subsequent time step 3 becomes $D^*_{i,3}$, which is summation of D_i, D_{i-1}, and D_{i-2} as illustrated in Eq. (3) below

$$D^*_{i,k} = \sum_{i=i-k+1}^{i=i} D_i; \qquad i \geq k; \quad i = 1, 2, \ldots, i; \quad k = 1, 2, \ldots, k \tag{3}$$

Due to different climate and soil properties in each region, the aggregated moisture departure can have different means and standard deviations. To minimize the geophysical discrepancy of soil moisture conditions, the aggregated moisture departure is then standardized to represent SODI in a general form associated with time window (k) at month (i) as follows:

$$\mathrm{SODI}_{i,k} = \frac{D^*_{i,k} - \bar{D}^*_k}{S_k} \tag{4}$$

where $\bar{D}^*_k$ and S_k = mean and the standard deviation of the aggregated moisture departure at time window k, respectively. It is possible that the aggregated moisture departure may follow skewed distribution due to various climates at different regions. When that is the case, the aggregated moisture departure distribution needs to be transformed into the normal distribution using the Box-Cox transformation method (Box and Cox 1964). SODI can be then defined as

$$\mathrm{SODI}_{i,k} = \frac{y_{i,k} - \bar{y}_k}{S_{y,k}} \tag{5}$$

$$y_{i,k} = \begin{cases} \frac{(D^*_{i,k} + \lambda_2)^{\lambda_1} - 1}{\lambda_1} & (\lambda_1 \neq 0), \\ \log(D^*_{i,k} + \lambda_2) & (\lambda_1 = 0) \end{cases} \tag{6}$$

where $y_{i,k}$ = transformed $D^*_{i,k}$ with mean $\bar{y}_k$ and standard deviation; and $S_{y,k}$; λ_1, λ_2 = Box-Cox transformation parameters.

The parameters can be easily computed by using *AID* software package for R environment. Note that the software package estimates Box-Cox transformation parameters by applying seven different normality tests. In this study, the Shapiro-Wilk normality test (Shapiro and Wilk 1965) was chosen to estimate λ_1 because this was the most reliable method among its peer group, including Kolmogorov-Smirnov test, Anderson-Darling test, and the Lilliefors test (Razali and Wah 2011). A normal range of SODI representing droughts is listed in Table 1.

Table 1. SODI Classification

SODI value	SODI category
SODI > 2	Extreme wet conditions
1.5 < SODI ≤ 2	Severe wet conditions
1 < SODI ≤ 1.5	Moderate wet conditions
0.5 < SODI ≤ 1	Mild wet conditions
−0.49 < SODI ≤ 0.5	Near normal
−1 < SODI ≤ −0.5	Mild drought
−1.5 < SODI ≤ −1	Moderate drought
−2 ≤ SODI ≤ −1.5	Severe drought
SODI < −2	Extreme drought

Moisture Departure (D) in PDSI and SPEI

Moisture departure (D_i) as used in this study is different from that used in PDSI and SPEI. In PDSI, D_i is defined as deficiency of precipitation and the expected precipitation for the given month (e.g., January), which represents the excess or shortage of precipitation compared to normal conditions for that month [see Eq. (17) in "Appendix"]. The moisture departure, D_i, in SPEI is instead simply defined as a functional relationship between precipitation and potential evapotranspiration to represent mechanisms of flux-in and flux-out processes for plant growth. SPEI does not take into account additional hydrological components, such as groundwater recharge, surface runoff, and loss from soil moisture. Storage capability of the soil is one of the most important factors that results in the slow development of drought. However, SPEI does not account for soil properties so that this leads to quick phase changes, particularly at shorter time scales (e.g., 1–6 month windows). Note that this deficiency can be faded by application of longer time scales (e.g., 12 months and longer)

$$D_i = P_i - \mathrm{PE}_i \tag{7}$$

where PE_i = potential evapotranspiration at time step, i.

Consequently, moisture departure in both PDSI and SPEI does not conceptualize month-to-month transitions. The previous month's conditions do not directly affect the moisture departure of the current month (D_i), which leads to a noncontinuous index with a large number of fluctuation and quick phase changes (from dry to wet or vice versa). Although duration factors defined by a linear regression over spatially adjusted moisture departure (z) are used in PDSI to address monthly transition of soil moisture, the continuity of this transition is not explicitly formulated. Thus, the moisture departure in January does not necessarily affect February's conditions. To resolve this issue, Palmer (1965) adopted climate characteristic coefficients, while Vicente-Serrano et al. (2010) used a statistical distribution function to represent hydrological conditions for an individual month.

Study Area and Data Used

To compare the performances between the newly developed drought index (SODI) and the others widely-used drought indices (SPI, sc-PDSI, and SPEI), various locations in the state of Idaho were selected as a study area based on the following reasons. First, it is anticipated that if the proposed drought index well represents droughts in Idaho, which is characterized by complicated terrain and land use, including forest, rangeland, and irrigated agriculture, broad applications of the index are likely. Second, a drought-prone area has been identified from Sohrabi et al. (2013) and the study area has experienced several droughts from 2000 to 2010 (except 2006) so that performance of the index can be easily evaluated

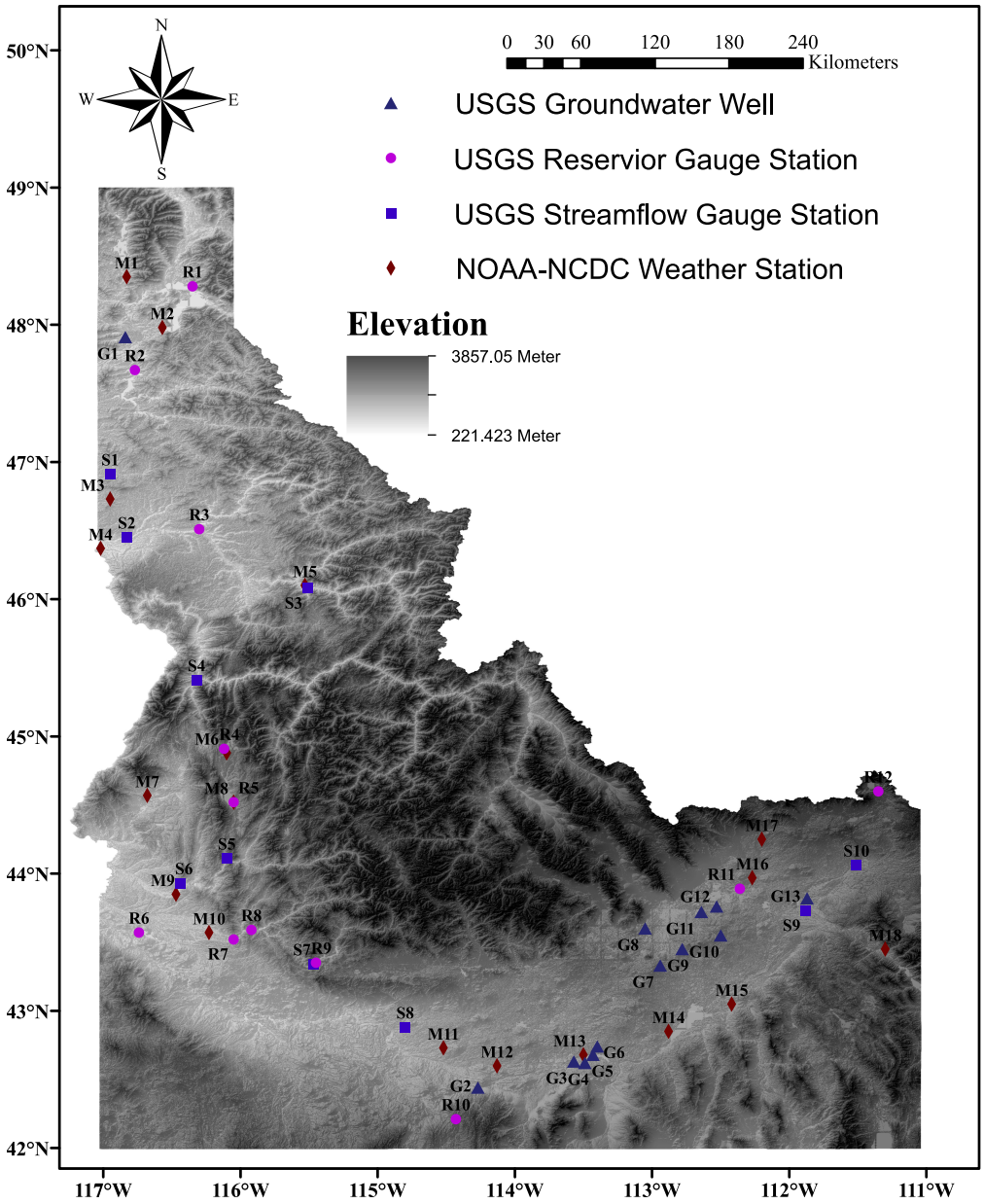

Fig. 2. Map of the selected hydro/climate data stations in Idaho, USA; G = groundwater station, R = reservoir storage, S = streamflow gauge station, W = weather station; USGS digital elevation model (DEM) was used with 1 arc-second resolution (data from USGS 2015)

through a verification process. As shown in Fig. 2, a total of 18 weather stations characterized by a long-term and high-quality dataset have been selected for this study. Since spatial comparison and trend analysis are not the goal of this work, stations with different period of records were used to maximize number of stations. All the stations used, which have less than 4% missing values in climatic parameters, such as precipitation and temperature, are listed in Table 2. The altitude of the weather stations (M) varies from 437.7 (Lewiston Nez Perce Co Airport at Station M4) to 1,661.2 m (Dubois Exp Station at Station M17) as shown in Fig. 2.

In addition, to promote the applicability of SODI at different climate regions, nine additional weather stations were selected across the states in the U.S. as shown in Fig. 3. Those include: Marine West Coast (also known as Oceanic Climate) which is also the predominant climate across the most parts of Europe (station C1), Mediterranean (C2), Midlatitude Desert (C3), Highland or Alpine (C4), Semi-Arid Steppe (C5), Humid Continental with warm summer (C6), Humid Continental with cool summer (C7), Humid Subtropical (C8), and Tropical (C9). These nine stations also cover wide range of altitudes (from 10 to 8,288 m) (Table 3).

Monthly precipitation and temperature data were retrieved from the National Climatic Data Center (NCDC) to compute sc-PDSI, SPI, SPEI, and SODI, while AWC was obtained from soil information for environmental modeling and ecosystem management at http://www.soilinfo.psu.edu.

Hydrological variables, including streamflow, reservoir storage, and groundwater level, are obtained from the U.S. Geological Survey (USGC) website (www.usgs.gov). As shown in Fig. 1, a total of 10 stream gauge stations (S), 12 reservoir storages (R), and 13 groundwater stations (G) located in the state of Idaho characterized by high quality and having at least 30 years of record were also used for cross-validation (also see Tables 8–10 of "Appendix" for details).

Table 2. Weather Stations (M) in the State of Idaho

Stations number	Station name	Coop-ID	Latitude	Longitude	Elevation	Percentage of missing in PRCP (%)	Percentage of missing in TEMP (%)	Period
M1	Priest River Exp Station	107,386	48.35	−116.83	725.4	0.16	0.02	1950–2010
M2	Bayview Model Basin	100,667	47.98	−116.57	632.5	3.51	2.28	1962–2010
M3	Moscow U Of I	106,152	46.73	−116.95	810.8	0.11	0.06	1950–2010
M4	Lewiston Nez Perce Co Airport	105,241	46.37	−117.02	437.7	2.74	2.23	1950–2010
M5	Fenn Rs	103,143	46.1	−115.53	475.5	2.82	3.72	1950–2010
M6	Mc Call	105,708	44.88	−116.1	1,531.6	0.71	0.65	1950–2010
M7	Cambridge	101,408	44.57	−116.68	807.7	0.42	0.3	1950–2010
M8	Cascade 1 NW	101,514	44.52	−116.05	1,492.3	0.67	0.62	1950–2010
M9	Emmett 2 E	102,942	43.85	−116.47	728.5	0.17	0.94	1950–2010
M10	Boise Air Terminal	101,022	43.57	−116.23	857.7	2.37	2.18	1950–2010
M11	Jerome	104,670	42.73	−114.52	1,140	0.6	0.44	1950–2010
M12	Hazelton	104,140	42.6	−114.13	1,237.5	0.82	1.34	1950–2010
M13	Minidoka Dam	105,980	42.68	−113.5	1,269.2	2.64	2.67	1962–2010
M14	American Falls 6 NE	100,227	42.85	−112.88	1,345.7	1.6	1.79	1962–2007
M15	Ft Hall 1 NNE	103,297	43.05	−112.42	1,360.9	2.14	2.87	1962–2007
M16	Hamer 4 NW	103,964	43.97	−112.27	1,460	1.68	3.57	1962–2007
M17	Dubois Exp Station	102,707	44.25	−112.2	1,661.2	0.1	0.06	1950–2010
M18	Swan Falls P H	108,928	43.45	−111.3	708.7	1.55	1.7	1950–2010

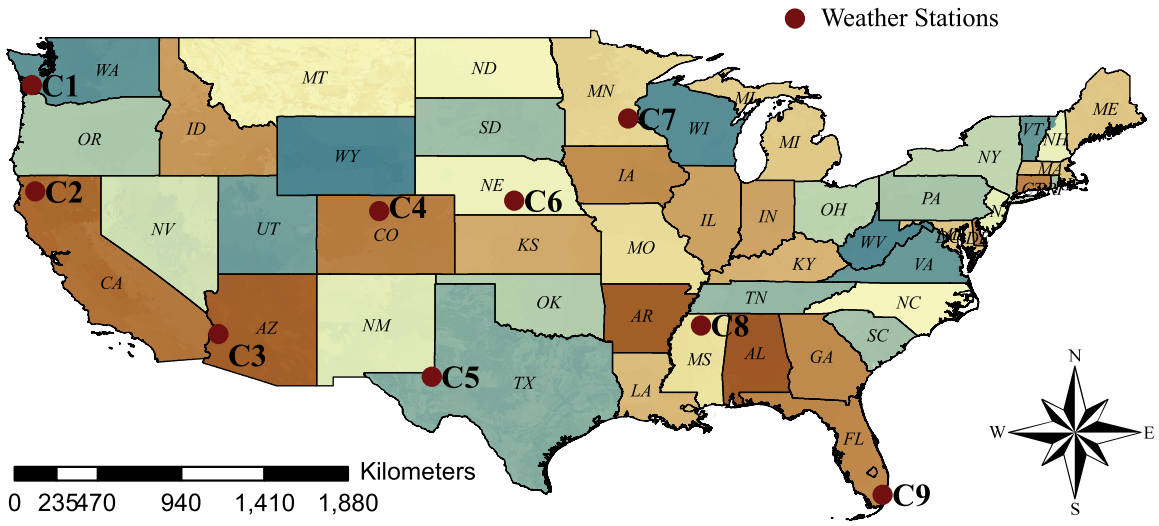

Fig. 3. Additional weather stations selected to verify SODI across the states in the U.S.

Table 3. Additional Weather Stations (C) across the States in U.S.

Stations number	Station name	Coop-ID	Latitude	Longitude	Elevation (m)
C1	Aberdeen, Washington	450008	46.58	−123.49	10
C2	Orleans, California	046508	41.18	−123.32	403
C3	Bouse, Arizona	020949	33.94	−114.02	925
C4	Grand Lake 6 SSW, Colorado	053500	40.18	−105.87	8,288
C5	Wink FAA Airport, Texas	419830	31.78	−103.20	2,807
C6	Kearney 4 NE, Nebraska	254335	40.72	−99.01	2,130
C7	Minneapolis WSFO Airport, Minnesota	215435	44.88	−93.23	872
C8	University, Mississippi	229079	34.37	−89.53	408
C9	Miami WSCMO Airport, Florida	085663	25.79	−80.32	29

Results

To assess the performance of the drought indices, a visual inspection was first carried out to compare results of the drought indices with historic drought records by visualizing onset, continuation, and termination of drought at the local level. Those indices were then correlated to hydrologic variables, including streamflow, reservoir storage, and groundwater level for cross-validation. The sensitivity of SODI was then evaluated through climate change scenarios for potential use of drought outlook indicators.

First Assessment: Drought Report

A comparison of the drought indices is illustrated in Fig. 4 in order to identify which index well represents dryness over time, as opposed to the historic drought records reported by the Idaho Bureau of Homeland Security (IBHS 2010). The report indicates that several droughts in 1960s and 1977 were recorded as the most severe single-year droughts in the state of Idaho. Two 2-year-long severe droughts are also reported in 1987–1988 and 1991–1992 followed by subsequent droughts during 2000–2010 except 2006.

Data from the weather station at Boise Air Terminal (M10 in Fig. 2) were primarily used to evaluate drought indices because this station has high quality and long-term data records. Since the temporal scale of sc-PDSI is typically a window of 9 to 12 month (Lloyd-Hughes and Saunders 2002; Vicente-Serano and Lopez-Moreno 2005), 12-month SODI, SPI, and SPEI were used for this comparison.

As shown in Fig. 4, the monthly variability of 12-month SODI is clearly less than that in the other drought indices as it attains soil moisture conditions at the previous time step for the next time step during index computation. In general, all indices indicate dry condition in late 1960s, but there are few discrepancies. The first discrepancy among the drought indices was observed in year 1977, where he 12-month SPI and SPEI represent a relatively short-term drought, while the 12-month SODI and sc-PDSI indicate severe and long-term droughts. Another observation was found during 1987–1991. The 12-month SODI, SPEI, and SPI well represent two 2-year-long droughts, but sc-PDSI overestimates droughts by indicating 8-year-long, very severe drought conditions. This pattern has been also observed in years 2000 through 2004. To verify how well SODI represents severe drought conditions at different climate zones, Station C5 in Texas is selected to evaluate the severe drought year 2011 in the state of Texas. Fig. 5 shows that all the drought indices detect the severe drought year 2011, the most

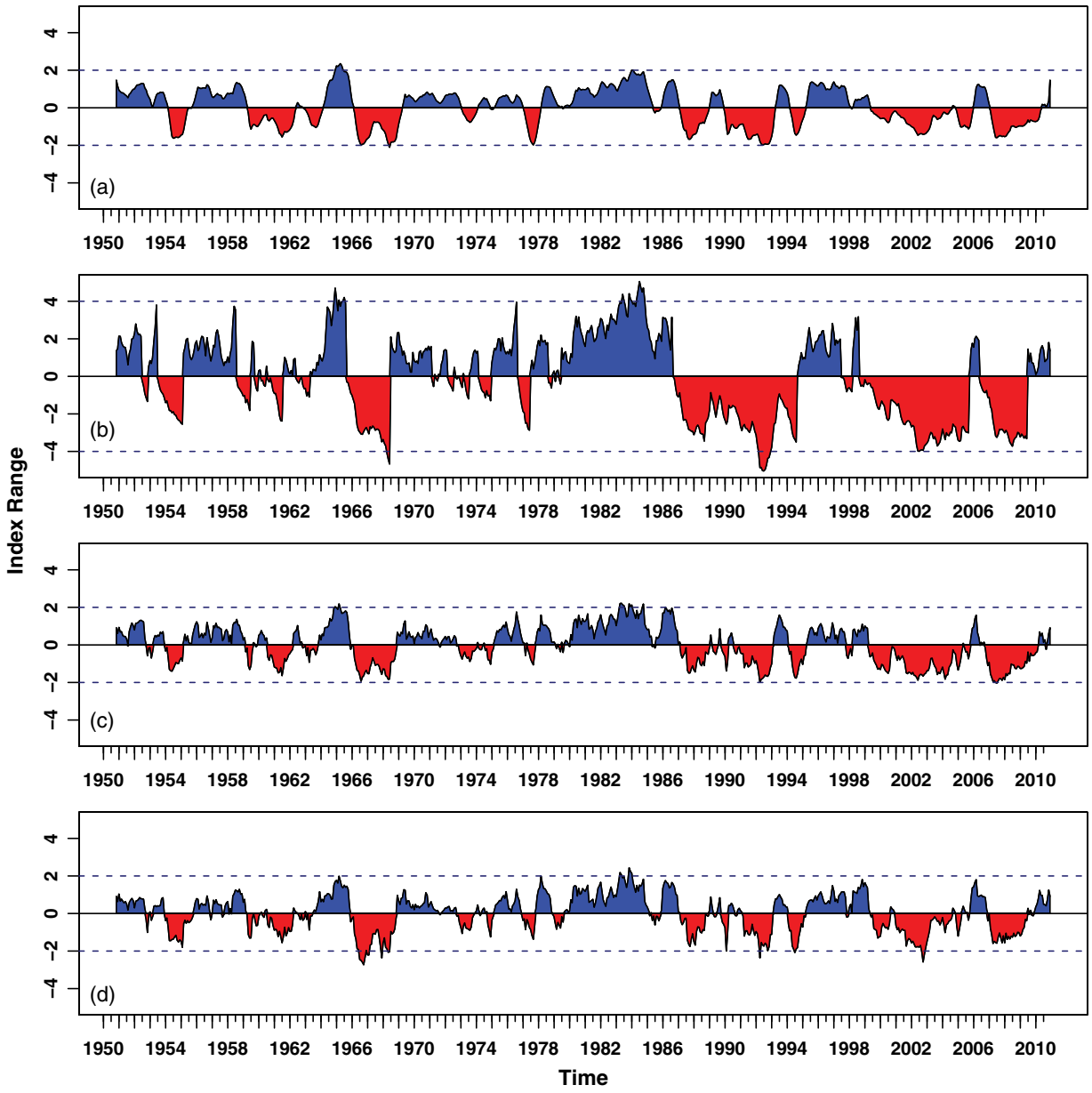

Fig. 4. Comparisons of the drought indices at Station M10 in Idaho: (a) 12-month SODI; (b) sc-PDSI; (c) 12-month SPEI; (d) 12-month SPI; horizontal dashed lines indicate extreme dry/wet conditions

J. Hydrol. Eng.

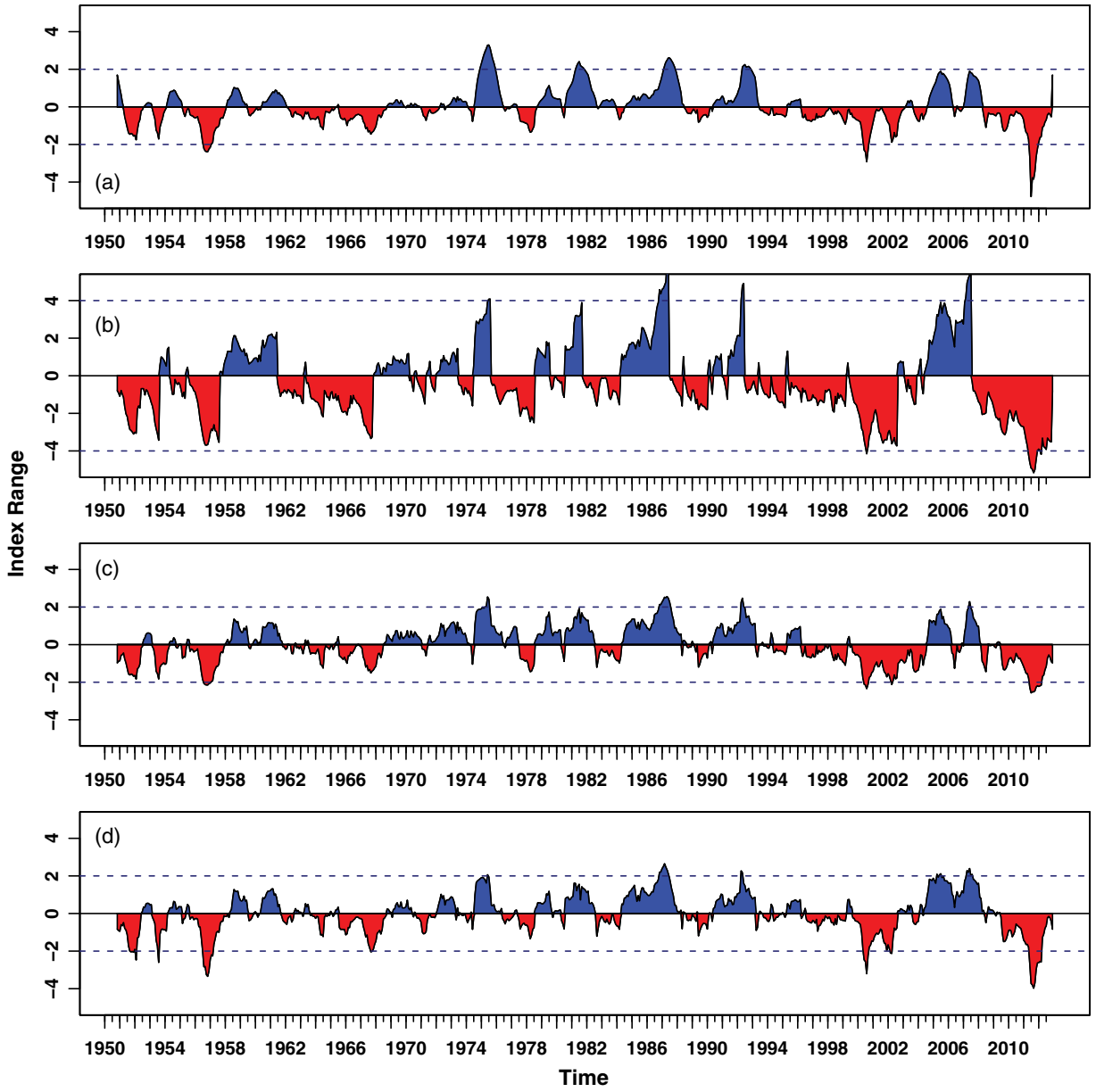

Fig. 5. Comparisons of the drought indices at Station C5 in Texas: (a) 12-month SODI; (b) sc-PDSI; (c) 12-month SPEI; (d) 12-month SPI; horizontal dashed lines indicate extreme dry/wet conditions

costly drought in history and the driest year on record reported by Texas A&M University's AgriLife Extension Office. The SODI and sc-PDSI are the only drought indices that identify 2011 distinctly as the driest year in the record. The sc-PDSI indicates that the 2011 drought initiated in 2007 after a sudden phase change from the previous years (from extreme wet condition to mild dry condition at the middle of 2007), while SODI shows that the 2011 drought began in 2008. For SODI, it took six month in transition from extreme wet condition to mild drought, which is more realistic [Fig. 5(a)]. A severe drought was also reported in the 1950s (Dunn 2010). The 1950s drought started in 1951 but was terminated two years later due to spring rainfall in 1953. This incident has been well captured by all drought indices except sc-PDSI.

Station C1in Washington was also investigated to evaluate how SODI represents drought in the Marine climate. Station C1 is located in Marine West Coast climate (Fig. 3), which is characterized by few extremes of temperature (mild summers and winters) and plenty of precipitation in all winter months. As shown in Fig. 6, time series of the drought indices are very similar to one another except a discrepancy observed for drought conditions in 1977, where sc-PDSI does not identify an extreme drought as the other indices do.

Second Assessment: Hydrological Characteristics

To verify how SODI can represent drought conditions associated with hydrologic variables, including streamflow, reservoir storage, and groundwater level, correlation coefficients between SODI and hydrological variables were computed at different spatial and time scales.

Streamflow

Hydrologic responses of drought depend on watershed characteristics determined by vegetation coverage, soil profile, and landscape type. In the mountain west area, however, snow melting is

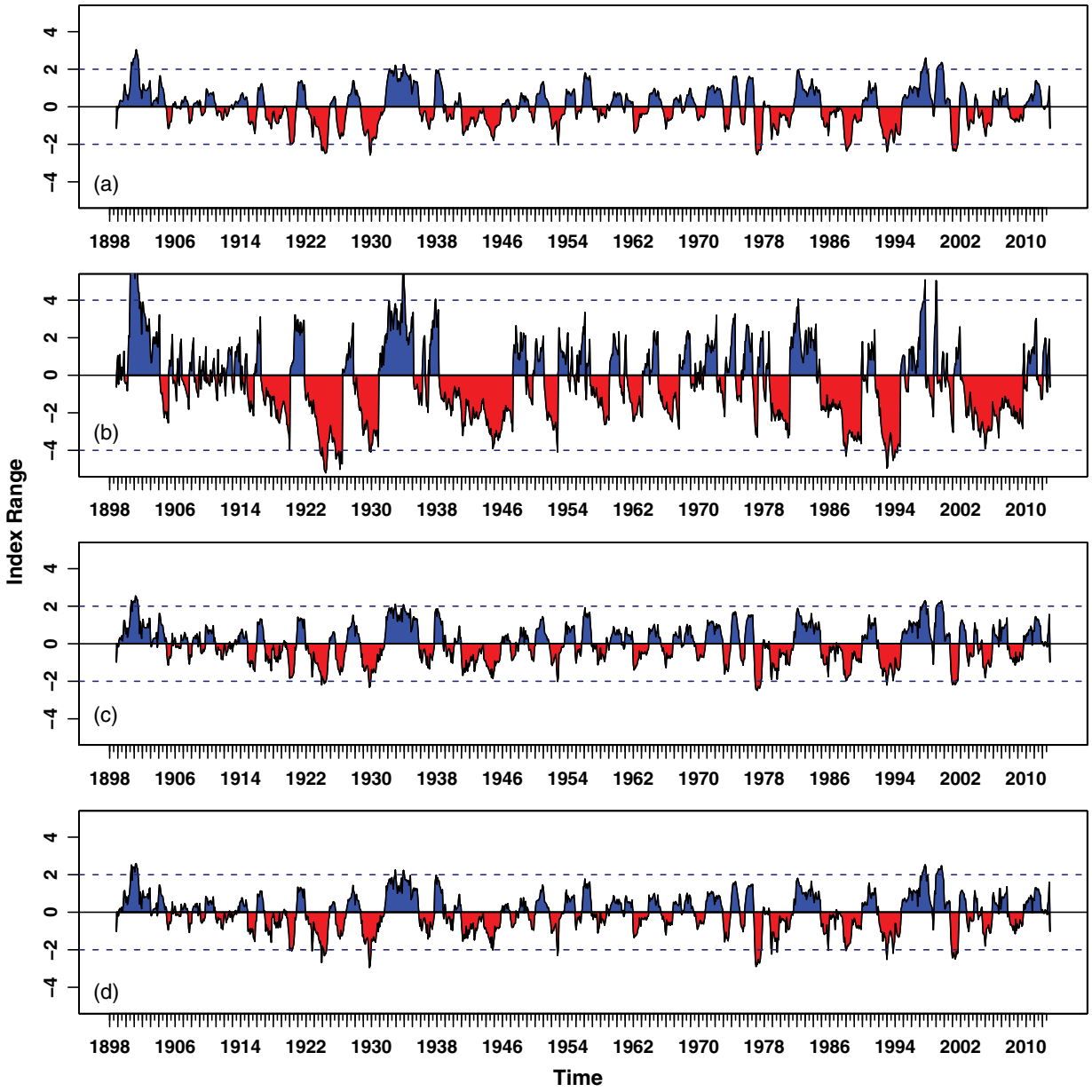

Fig. 6. Comparisons of the drought indices at Station C1 in Washington: (a) 12-month SODI; (b) sc-PDSI; (c) 12-month SPEI; (d) 12-month SPI; horizontal dashed lines indicate extreme dry/wet conditions

a key factor that has profound influence on streamflow augmentation. It is expected that response time between rainfall-runoff processes is relatively slow in the snow-dominated watershed. Thus, since highest streamflow occurs sometime between midspring through early summer when snow starts to melt, short time scales (e.g., 1–6 months) of drought indices may be well correlated to snow-melting runoffs.

As shown in Table 4, correlation coefficients between streamflow and drought indices increases as time scale increases. For SPEI and SPI, the highest correlation was identified at 6-month and 12-month time scales at all the stations, respectively. However, for SODI, the highest correlation can be found at 1-month, 3-month or 6-month time scales. For instance, the highest correlation between streamflow and SODI at a 1-month time window was found at Station S1, and that for a 3-month time window was found at Stations S2 and S6. This result may be affected by various factors such as moisture storage of soil, infiltration rate, and distance of the stations to the head water.

Table 4. Correlation Coefficients between Drought Indices and Flow at Stream Gauge Stations (S)

Station number	1-Month			3-Month			6-Month		
	SODI	SPEI	SPI	SODI	SPEI	SPI	SODI	SPEI	SPI
S1	0.70	0.46	0.26	0.64	0.65	0.27	0.27	0.67	0.27
S2	0.50	0.09	0.09	0.56	0.33	0.14	0.48	0.68	0.19
S3	0.21	−0.01	0.04	0.39	0.19	0.11	0.66	0.57	0.17
S4	0.37	−0.09	0.06	0.54	0.12	0.11	0.67	0.58	0.21
S5	0.07	−0.29	0.12	0.38	−0.08	0.23	0.66	0.35	0.30
S6	0.55	−0.01	0.10	0.61	0.23	0.18	0.51	0.60	0.28
S7	0.20	−0.29	0.04	0.45	−0.02	0.10	0.62	0.40	0.21
S8	0.47	0.03	0.10	0.52	0.18	0.17	0.52	0.45	0.32
S9	0.23	−0.18	0.06	0.32	0.11	0.13	0.33	0.48	0.21
S10	0.25	0.04	0.09	0.39	0.21	0.13	0.53	0.42	0.19
Average	0.354	−0.03	0.09	0.481	0.12	0.12	0.52	0.52	0.24
Diff[a]	NA	0.38	0.23	NA	0.29	0.32	NA	0.00	0.29

[a]Indicate that the difference of SPEI and SPI correlation coefficient from SODI.

Table 5. Correlation Coefficients between Drought Indices and the Streamflow-Based Hydrological Drought Index (HDI), from Ryu et al. (2010) at Stream Gauge Stations (S)

Station number	1-Month			3-Month			6-Month			12-Month		
	SODI	SPEI	SPI	SODI	SPEI	SPI	SODI	SPEI	SPI	SODI	SPEI	SPI
S1	0.87	0.66	0.26	0.90	0.70	0.31	0.88	0.65	0.40	0.76	0.75	0.71
S2	0.54	0.13	0.11	0.53	0.06	0.18	0.48	−0.01	0.24	0.63	0.58	0.53
S3	0.39	0.08	0.13	0.36	−0.07	0.16	0.30	−0.18	0.21	0.65	0.60	0.57
S4	0.53	−0.05	0.12	0.57	−0.17	0.17	0.55	−0.24	0.22	0.63	0.57	0.53
S5	0.00	−0.41	0.11	0.02	−0.45	0.18	0.12	−0.34	0.29	0.58	0.51	0.50
S6	0.60	0.00	0.13	0.62	−0.05	0.22	0.61	−0.05	0.31	0.60	0.56	0.55
S7	0.05	−0.34	0.03	0.06	−0.42	0.07	0.16	−0.41	0.20	0.60	0.47	0.44
S8	0.41	−0.06	0.16	0.49	−0.08	0.20	0.62	0.02	0.30	0.74	0.55	0.49
S9	0.24	−0.31	0.08	0.26	−0.34	0.04	0.28	−0.28	0.12	0.41	0.44	0.34
S10	0.20	−0.03	0.08	0.23	−0.03	0.12	0.30	0.04	0.20	0.53	0.47	0.46
Average	0.37	−0.02	0.12	0.40	−0.07	0.17	0.43	−0.05	0.26	0.61	0.55	0.51
Diff[a]	NA	0.39	0.25	NA	0.46	0.23	NA	0.48	0.18	NA	0.06	0.10

[a]Indicate that the difference of SPEI and SPI correlation coefficient from SODI.

Overall, the highest correlation was observed from SODI, except at S2 and S9 at a 6-month window (Table 4). In general, SODI explained 7.5 and 8.5% more variance (difference in correlation coefficient) than t SPEI and SPI, respectively. SPEI shows negative correlation of a 1-month window at most stations because evapotranspiration is small during the winter, while maximum discharge occurs sometime between midspring through early summer due to snow melting processes. This also implies that short-term SPEI is not a plausible indicator to represent streamflow-driven hydrological drought to the same extent as SODI.

Correlation coefficients between the drought indices and the streamflow-based hydrological drought index [e.g., HDI, Ryu et al. (2010)] show similar results. The highest correlation is related to SODI, except at S9 (Table 5). Roughly, SODI explains 15 and 4% more variance than SPEI and SPI, respectively.

Reservoir Storage

Short and midrange drought (e.g., 3–12 months) indices well responded to variations of reservoir storage. It appears that the highest correlation was observed at SODI for storage-driven hydrological drought (Table 6). The results indicate that SODI can explain 4.7 and 4.4% more variance than SPEI and SPI, respectively.

Groundwater Level

Drought condition in midterm to long-term (e.g., 12–48 months) is well represented by groundwater variations as shown in Table 7. As time windows expand, the drought indices better represent variations in groundwater levels. Thus, higher correlation coefficients were observed at 48-month time scales.

Negative correlation coefficients between the drought indices and groundwater level have been observed at all locations because groundwater level is measured as the depth of the water level below the land surface. As shown in Table 7, the 12-month and 24-month SPI values have higher correlation coefficients at G3, G4, G5, and G6. The 36-month SPI also shows higher correlation at G4, G5, and G6 than others. It appears that SODI explains 0.3 and 0.4% more variance than SPEI and SPI, respectively. This result also indicates that the highest correlation coefficients at all the groundwater stations are associated with SODI, except at G6 (Table 7).

Global Warming Scenarios

To evaluate the sensitivity of SODI to changes in temperature and precipitation, two global warming scenarios similar to Vicente-Serrano et al. (2010) were employed in this study.

Progressive Air Temperature Increase (Case 1)

Observed temperature data were perturbed to represent hydrologic cycles induced by climate change (Ryu et al. 2011). A 2°C increment of temperature increase was applied to each weather station. Then, drought indices were calculated using the perturbed temperature. The drought index calculated from this global warming scenario is denoted as 2T. For instance, the 12-month SODI associated with temperature increases of 2°C is denoted as 12-month SODI-2T.

Progressive 15% Decrease of Precipitation (Case 2)

Observed precipitation data were altered by multiplying an adjustment factor of 0.85 (15% decrease). Drought indices associated with this scenario are then computed and denoted as P extension (i.e., 12-month SODI-P). Since a progressive nature can be induced by global warming scenarios, climate variability and change is considered to increase temperatures and decrease precipitation.

Fig. 7 indicates how well the 12-month SODI responds to changes in temperature, precipitation, and climate change at Station M10 in Idaho. As shown in Fig. 7, under global warming scenarios, the magnitude and duration of droughts increase over time. For instance, 12-month SODI well captured drought conditions in 1977

Table 6. Correlation Coefficients between Drought Indices and Reservoir Storage (R)

Station number	3-Month			6-Month			12-Month		
	SODI	SPEI	SPI	SODI	SPEI	SPI	SODI	SPEI	SPI
R1	−0.29	−0.66	0.19	0.25	−0.23	0.18	0.12	0.13	0.13
R2	−0.06	−0.18	0.22	0.31	0.17	0.22	0.20	0.21	0.18
R3	−0.05	−0.30	−0.18	0.18	−0.10	−0.07	−0.10	−0.17	−0.18
R4	0.05	−0.49	0.08	0.53	0.02	0.03	0.03	0.05	0.05
R5	0.15	−0.20	0.15	0.46	0.11	0.22	0.42	0.39	0.37
R6	0.62	0.51	0.07	0.71	0.71	0.14	0.33	0.15	0.20
R7	0.28	−0.26	0.04	0.63	0.28	0.02	0.15	0.12	0.13
R8	0.69	0.60	0.11	0.44	0.68	0.15	0.28	0.26	0.26
R9	0.09	−0.24	0.07	0.41	0.03	0.15	0.52	0.44	0.40
R10	0.57	0.10	0.14	0.67	0.39	0.25	0.62	0.50	0.46
R11	0.49	0.38	0.10	0.45	0.47	0.14	0.19	0.19	0.19
R12	0.44	0.18	0.13	0.48	0.37	0.25	0.55	0.52	0.44
Average	0.25	−0.05	0.09	0.46	0.24	0.14	0.28	0.23	0.22
Diff[a]	NA	0.30	0.16	NA	0.22	0.32	NA	0.04	0.06

[a]Indicate that the difference of SPEI and SPI correlation coefficient from SODI.

(retrospective drought outlooks) as well as transition periods from wet to dry conditions seen during 1993–1994 [Fig. 7(a)]. As expected, the magnitude of drought increases when global warming scenarios are applied [Figs. 7(b and c)]. Thus, as shown in Fig. 7, the year of 2006 was identified as a wet year, but the magnitude of this wet year was reduced noticeably under global change with temperatures increased and precipitation decreased.

Figs. 8 and 9 show differences between drought indices associated with global change scenarios to evaluate how drought indices respond to global warming and their sensitivity to variations in

Table 7. Correlation Coefficients between Drought Indices and Groundwater Level (G)

Station number	12-Month			24-Month			36-Month			48-Month		
	SODI	SPEI	SPI	SODI	SPEI	SPI	SODI	SPEI	SPI	SODI	SPEI	SPI
G1	−0.57	−0.53	−0.50	−0.79	−0.77	−0.75	−0.86	−0.85	−0.84	−0.84	−0.83	−0.84
G2	−0.36	−0.04	0.06	−0.40	−0.16	−0.03	−0.47	−0.27	−0.11	−0.50	−0.36	−0.18
G3	−0.36	−0.31	−0.39	−0.40	−0.33	−0.42	−0.45	−0.36	−0.43	−0.49	−0.41	−0.45
G4	−0.36	−0.34	−0.40	−0.40	−0.37	−0.44	−0.46	−0.41	−0.47	−0.51	−0.46	−0.50
G5	−0.36	−0.33	−0.40	−0.42	−0.39	−0.46	−0.48	−0.44	−0.49	−0.53	−0.49	−0.52
G6	−0.22	−0.22	−0.24	−0.27	−0.32	−0.34	−0.34	−0.43	−0.45	−0.40	−0.55	−0.58
G7	−0.22	−0.18	−0.19	−0.35	−0.30	−0.32	−0.44	−0.40	−0.42	−0.54	−0.50	−0.52
G8	−0.13	−0.12	−0.12	−0.17	−0.15	−0.16	−0.19	−0.18	−0.19	−0.20	−0.19	−0.19
G9	−0.20	−0.16	−0.17	−0.33	−0.27	−0.30	−0.45	−0.40	−0.43	−0.57	−0.52	−0.55
G10	−0.24	−0.19	−0.15	−0.34	−0.27	−0.24	−0.41	−0.35	−0.33	−0.47	−0.42	−0.41
G11	−0.21	−0.11	−0.01	−0.32	−0.21	−0.08	−0.39	−0.30	−0.13	−0.49	−0.39	−0.20
G12	−0.32	−0.25	−0.20	−0.43	−0.36	−0.31	−0.53	−0.46	−0.42	−0.58	−0.52	−0.50
G13	−0.11	−0.08	−0.09	−0.12	−0.10	−0.11	−0.12	−0.09	−0.11	−0.10	−0.08	−0.08
Average	−0.28	−0.22	−0.22	−0.36	−0.31	−0.30	−0.43	−0.38	−0.37	−0.48	−0.44	−0.42
Diff[a]	NA	0.06	0.06	NA	0.05	0.06	NA	0.05	0.06	NA	0.04	0.06

[a]Indicate that the difference of SPEI and SPI correlation coefficient from SODI.

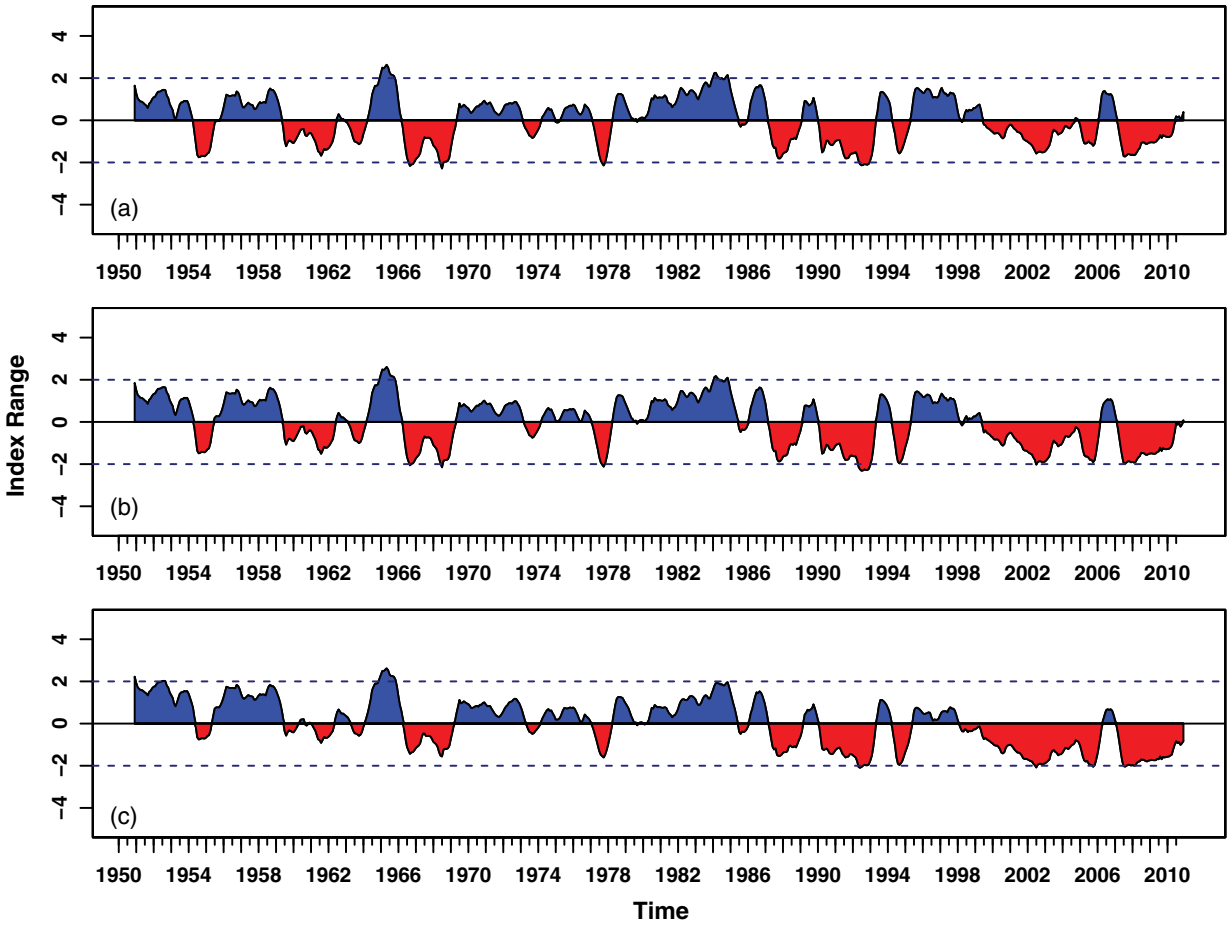

Fig. 7. Comparisons of the climate-induced 12-Month SODIs at Station M10 in Idaho: (a) 12-month SODI; (b) 12-month SODI−2 T; (c) 12-month SODI−P

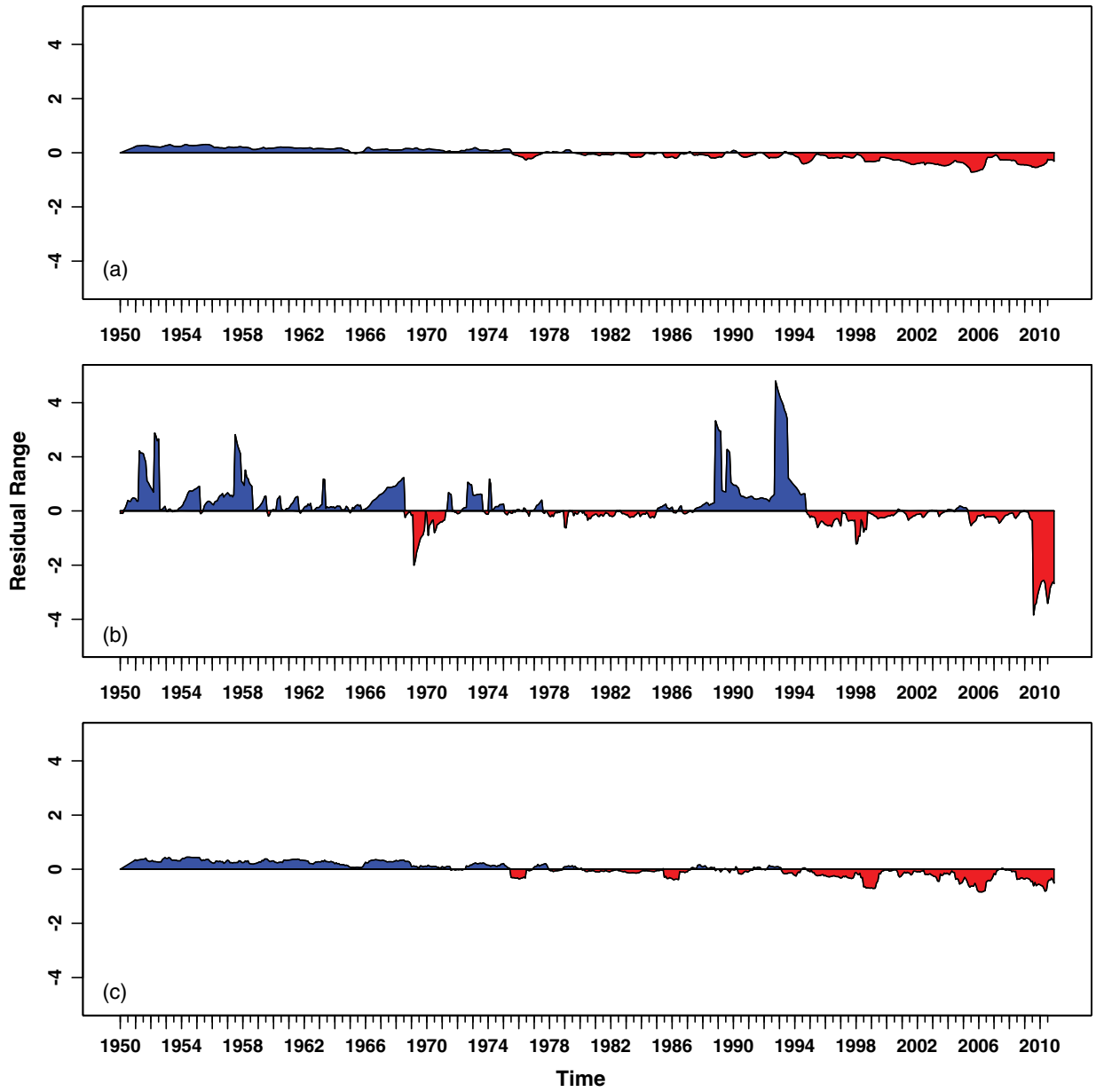

Fig. 8. Residual of drought indices associated with a 2°C temperature increase at Station M10 in Idaho: (a) residual of 12-month SODI; (b) residual of sc-PDSI; (c) residual of 12-month SPEI

perturbed precipitation and temperature. As shown in Fig. 8, the first 20 years have noticeably wetter condition even when a 2°C increase of the temperature was applied. As time passes, however, drought indices fairly represent drought evolution over time.

The 12-month SODI, in particular, well represents the progressive nature of drought by accounting for soil moisture conditions in the previous time step. As such, no noticeable spikes during month-to-month transitions were found. By contrast, sc-PDSI shows a number of spikes in the mid-1990s, and SPEI indicates a more rapid phase change (from dry to wet conditions, or vice versa) because no soil moisture is incorporated into their computation formula (Fig. 8). Fig. 9 compares the performance between the 12-month SODI–P and other indices associated with global change scenarios (Case 2). Unlike other drought indices, SODI well capture variations of 15% decreased precipitation induced by global change, perhaps due to sufficient moisture contribution in PET processes. As a result, SODI well represents drought characteristics induced by climate scenarios. This finding also agrees well with the study by Paulo et al. (2012) in that SODI reacts more evidently to the variability of precipitation than either SPI and SPEI during hydrological processes associated with soil moisture departure.

Summary and Conclusions

This study proposes a new drought index termed the "soil moisture drought index (SODI)," which can complement weakness of the existing drought indices. SODI can capture variations in precipitation and temperature and accounts for soil moisture characteristics over time. SODI meets all the requirements for a robust drought index indicated by Keyantash and Dracup (2002) in the sense that it can be easily computed using limited datasets. Additionally, the results show that SODI detects and quantifies extended severe

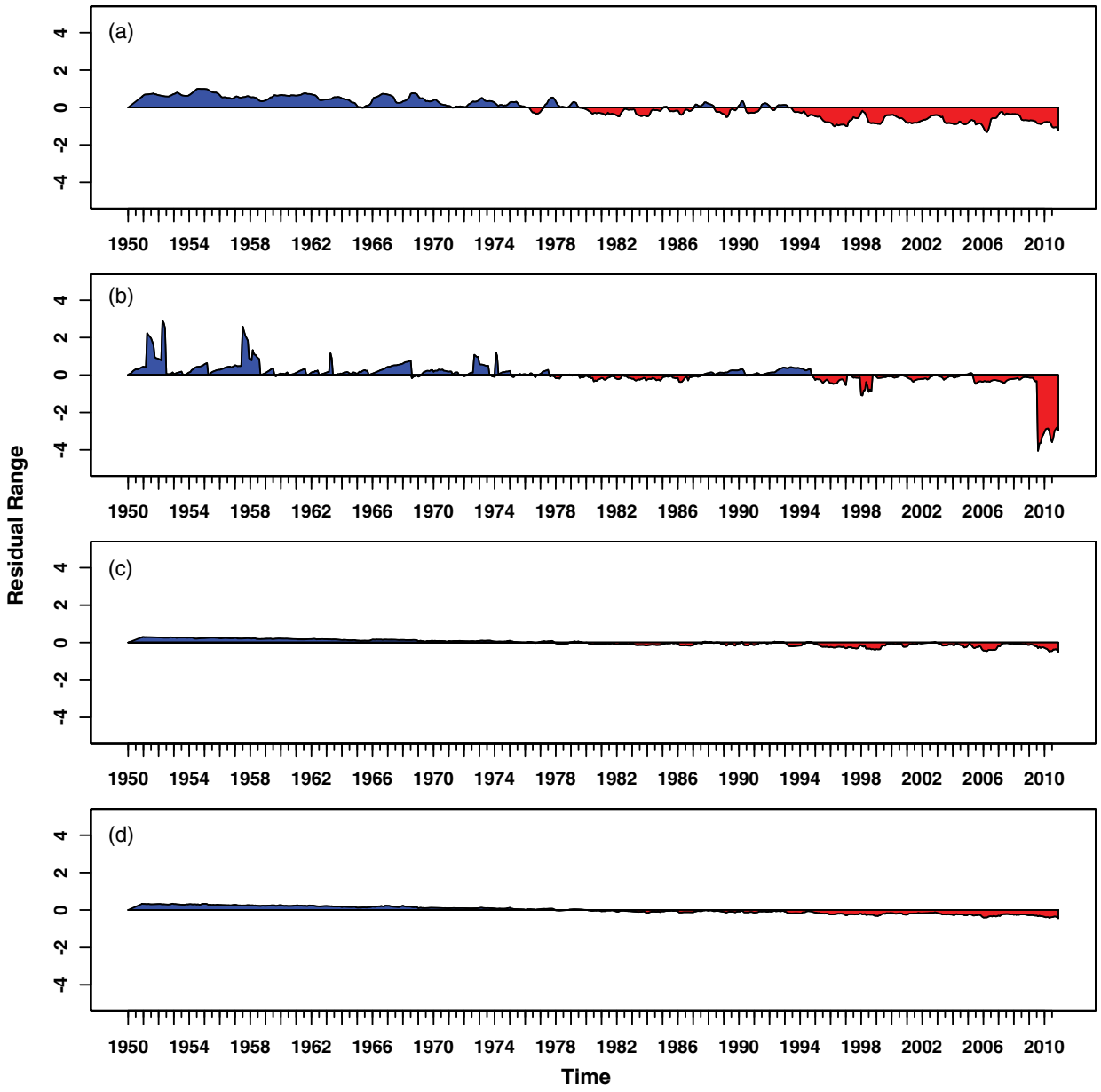

Fig. 9. Residual of drought indices associated with a 15% precipitation decrease at Station M10 in Idaho: (a) residual of 12-month SODI; (b) residual of sc-PDSI; (c) residual of 12-month SPEI; (d) residual of SPI

droughts more accurately according to a comparison with the historic drought records published by the responsible agency (IBHS 2010).

Several discrepancies were highlighted among drought indices to evaluate which drought indices represent droughts well. In addition to drought evaluation based on drought reports, the performance of the drought indices was also evaluated by correlating them to hydrological variables, including streamflow, reservoir storage, and groundwater level. The result shows that proper consideration of time-dependent soil characteristics encapsulated in SODI can better characterize moisture dynamics, which is critical component to determine dryness during month-to-month transitions. However, discrepancies between SODI, SPI, and SPEI in some regions where supply (precipitation) is significantly larger than demand (evapotranspiration), such as Marine West Coast climate (C1), would be relatively small because soil water retention in such wet regions does not often lead to drought conditions.

Another interesting finding from this research is that 1–3 month SPEI is not plausible to represent hydrological droughts, especially for snow-dominated watersheds. Climate change scenarios applied in this study demonstrate that the capability of SODI corresponding to future climates is plausible.

In conclusion, SODI is a useful index to detect onset, continuation, and termination of droughts. An advantage of SODI against other indices is that SODI is a time-dependent and continuous index by characterizing soil moisture conditions during time transitions from the current time step to the next. Identifying the slow onset and termination of drought characterized by soil moisture departure, in particular, is critical to define drought for arid and semi-arid regions where agriculture is dominant. Since SODI is very flexible across space and time, there is potential to visualize drought maps in different time scales (e.g., 1-month, 3-month, 6-month, and 12-month) at multiple resolutions (e.g., local, regional, and national). By knowing SODI's performance associated with

climate change scenarios, SODI is considered to add momentum to build a case toward the use of soil moisture information for drought analysis in a changing environment.

Appendix. Brief Overview of sc-PDSI/PDSI

The self-calibrated PDSI (sc-PDSI) is an improved version of PDSI (Wells et al. 2004) that incorporates multiple environmental variables, including temperature (T), precipitation (P), actual/potential evapotranspiration (ET/PE), actual/potential runoff (RO/PRO), actual/potential recharge (R/PR), and actual/potential loss (L/PL). These variables except T and P need to be computed prior to the final index values.

Thornthwaite's method (Thornthwaite 1948) was used to calculate PE and other variables including, ET, RO, PRO, R, PR, L, and PL, which are estimated regarding to the following assumptions: (1) there is no moisture loss from the underlying layer unless the surface layer is completely dry; (2) evapotranspiration can take soil moisture of the surface layer without any limitation, while the loss from the underlying layer is proportional to the ratio of moisture content and AWC of this layer; (3) there is no recharge to the underlying layer until the surface layer is completely full (at field capacity); and (4) runoff occurs when both layers reach their combined AWC. Thus, runoff includes runoff and soil water content between field capacity (FC) and saturated point. Then, calculation procedure for a monthly time step is conducted as follows:

$$L_s = S_s' \quad \text{or} \quad (\text{PE} - \text{P}) \text{ whichever is smaller} \tag{8}$$

where L_s = moisture loss from the surface layer; and S_s' = available moisture stored in the surface layer at start of month

$$L_u = (\text{PE} - \text{P} - L_s)\frac{S_u'}{\text{AWC}} \tag{9}$$

where L_u = moisture loss from the underlying layer; S_u'= available moisture stored in the underlying layer at start of month; and AWC = combined available capacity of both layers. Thus, potential loss (PL) is

$$\text{PL} = \text{PL}_s + \text{PL}_u \tag{10}$$

where PL_s = potential loss from the surface layer; and PL_u = potential loss from the underlying layer. PL_s and PL_u are calculated as follows:

$$\text{PL}_s = \text{PE} \quad \text{or} \quad S_s' \text{ whichever is smaller} \tag{11}$$

$$\text{PL}_u = (\text{PE} - \text{PL}_s)\frac{S_u'}{\text{AWC}} \tag{12}$$

Potential recharge (PR) is then defined as the amount of moisture needed to bring soil moisture to field capacity, so we have

$$\text{PR} = \text{AWC} - S' \tag{13}$$

where S' = amount of available moisture in both layers at the beginning of the month. Then, potential runoff is defined as

$$\text{PRO} = \text{AWC} - \text{PR} \tag{14}$$

Consequently, actual evapotranspiration (ET) can be defined as

$$\text{ET} = \begin{cases} \text{P} + S' - S & \text{PE} > \text{P} \\ \text{PE} & \text{PE} < \text{P} \end{cases} \tag{15}$$

where S = available moisture in both layers at the end of the month. After conducting soil water balance for a desired period, climatically appropriate for existing condition coefficients (CAFEC) can be estimated as

$$\alpha = \frac{\overline{\text{ET}}}{\overline{\text{PE}}}, \qquad \beta = \frac{\bar{\text{R}}}{\overline{\text{PR}}}, \qquad \gamma = \frac{\overline{\text{RO}}}{\overline{\text{PRO}}} \quad \text{and} \quad \delta = \frac{\bar{\text{L}}}{\overline{\text{PL}}} \tag{16}$$

where α, β, γ, and δ = CAFEC coefficients for evapotranspiration, recharge, runoff and moisture loss, respectively. The bar over each parameter indicates average of that parameter over the given month.

D_i is defined as deficiency of precipitation and the expected precipitation for the given month of year (e.g., January), which represents the excess or shortage of precipitation compared to normal conditions for a month, shown in Eq. (17)

$$D_i = P_i - \hat{P}_j \tag{17}$$

where D_i = moisture departure at month i; P_i = precipitation at month i; and $\hat{P}_j$ = expected precipitation to maintain normal soil moisture condition for the given month, j (e.g., January, February and etc.) and defined as

$$\hat{P}_j = \widehat{\text{ET}}_j + \hat{R}_j + \widehat{\text{RO}}_j - \hat{L}_j \tag{18}$$

where ˆ indicates the expected value for each parameter for the given month j, which are estimated as follows:

$$\widehat{\text{ET}} = \alpha\text{PE} \tag{19}$$

$$\hat{\text{R}} = \beta\text{PR} \tag{20}$$

$$\widehat{\text{RO}} = \gamma\text{PRO} \tag{21}$$

$$\hat{\text{L}} = \delta\text{PL} \tag{22}$$

The moisture departure resulted from Eq. (17), D_i, merely shows deviation of precipitation from the expected precipitation. Therefore, the D values at different locations do not necessarily have the same values. To solve this issue, climate characteristic coefficient, K, and moisture anomaly index, Z, were defined by Palmer (1965) as follows:

$$K = \frac{17.67K'}{\sum_1^{12} \bar{D}K'} \tag{23}$$

where $\bar{\text{D}}$ = average monthly absolute values of D; and k' is a weighting factor defined as

$$k' = \log_{10}\left[\left(\frac{(\overline{\text{PE}} + \bar{\text{R}} + \overline{\text{RO}})}{(\bar{\text{P}} + \bar{\text{L}})} + 2.8\right)\Big/\bar{D}\right] + 0.5 \tag{24}$$

$$Z_i = D_i K \tag{25}$$

Furthermore, the moisture anomaly index, Z, does not conceptualize month-to-month transitions. For instance, the Z value in January does not necessarily affect the Z value of February. To solve this, Palmer (1965) defined duration factors (p and q) by using a linear regression over moisture anomaly index, which can be written as

$$X_i = 0.897X_{i-1} + \left(\frac{1}{3}\right)Z_i \tag{26}$$

where 0.897 and 1/3 are duration factors (p and q, respectively); and X is a PDSI value.

Duration factors, p and q, and climate characteristic coefficient, K, are empirical constants derived by Palmer (1965) using data from nine different locations. Wells et al. (2004) revised these empirical constants in a way that k, p, and q can be automatically estimated based on the historical climatic data of a location. Thus, Eqs. (23) and (26) can be replaced by Eqs. (27) and (28), respectively

$$K = \begin{cases} k'\left(-\frac{4}{\text{2nd percentile of PDSI}}\right), & \text{If } D < 0 \\ k'\left(\frac{4}{\text{98th percentile of PDSI}}\right), & \text{If } D \geq 0 \end{cases} \tag{27}$$

$$X_i = pX_{i-1} + qZ_i \tag{28}$$

$$p = \left(1 - \frac{m}{m+b}\right) \tag{29}$$

$$q = \frac{C}{m+b} \tag{30}$$

where C = calibration factor. Wells et al. (2004) assigned −4 and +4 for C to calibrate dry and wet conditions, respectively. The variables p and q are defined by linear regressions that separately fit over extreme dry and wet conditions in that dry and wet conditions can have different values for p and q at any particular location. Slope and intercept of these regression lines are m and b, respectively. Also see Tables 8–10 for the selected stations for cross-validation.

Table 8. Streamflow Gauge Stations

Station number	Hydrologic unit	River/gauge name	Station identifier	Latitude	Longitude
S1	13345000	Palouse River near Potlatch	106152	46.91	−116.95
S2	13342500	Clearwater River at Spalding	105241	46.45	−116.83
S3	13336500	Selway River near Lowell	103143	46.08	−115.51
S4	13316500	Little Salmon River at Riggins	101408	45.41	−116.32
S5	13246000	NF Payette River near Banks	101514	44.11	−116.1
S6	13249500	Payette River near Emmett	102942	43.93	−116.44
S7	13190500	SF Boise River below Anderson Ranch Dam	101022	43.34	−115.47
S8	13152500	Malad River near Gooding	104670	42.88	−114.8
S9	13038500	Snake River at Lorenzo	108928	43.73	−111.88
S10	13046000	Henrys Fork near Ashton	103964	44.06	−111.51

Table 9. Reservoir Storage

Station number	Hydrologic unit	Reservoir or lake name	Station identifir	Latitude	Longitude
R1	12392500	Lake Pend Oreille near Hope	107386	48.28	−116.35
R2	12415500	Lake Coeur d'Alene	100667	47.67	−116.77
R3	13340950	Dworshak reservoir near Ahsahka	106152	46.51	−116.3
R4	13238500	Payette Lake at McCall	105708	44.91	−116.12
R5	13244500	Cascade reservoir at Cascade	101514	44.52	−116.05
R6	13203500	Lake Lowell near Caldwell	101022	43.57	−116.74
R7	13201500	Lucky peak	101022	43.52	−116.05
R8	13194000	Arrowrock reservoir at Arrowrock Dam	101022	43.59	−115.92
R9	13190000	Anderson Ranch reservoir at Anderson Ranch Dam	101022	43.35	−115.45
R10	13106500	Salmon River Canal Co reservoir near Rogerson	104670	42.21	−114.43
R11	13115000	Mud Lake	103964	43.89	−112.36
R12	13039000	Henrys Lake	102707	44.6	−111.35

Table 10. Groundwater Gauge Stations

Station number	Hydrologic unit	County	Station identifier	Latitude	Longitude
G1	17010305	Kootenai County	107386	47.91	−116.84
G2	17040212	Twin Falls County	104140	42.44	−114.27
G3	17040209	Cassia County	105980	42.63	−113.57
G4	17040209	Cassia County	105980	42.62	−113.49
G5	17040209	Blaine County	105980	42.68	−113.43
G6	17040209	Blaine County	100227	42.74	−113.4
G7	17040206	Bingham County	103297	43.33	−112.94
G8	17040201	Bonneville County	103964	43.6	−113.05
G9	17040206	Bingham County	103297	43.45	−112.78
G10	17040206	Bonneville County	103964	43.55	−112.5
G11	17040206	Jefferson County	102707	43.72	−112.64
G12	17040215	Jefferson County	103964	43.76	−112.53
G13	17040204	Madison County	103964	43.82	−111.87

Acknowledgments

The authors would like to acknowledge Idaho Water Resources Research Institute (IWRRI) for providing USGS 104B grant support for this study. The SODI software will be available at http://water.cals.uidaho.edu once it is completed.

References

AID version 1.4 [Computer software]. Vienna, Austria, ⟨http://CRAN.R-project.org/package=AID⟩.

Alley, W. M. (1984). "The Palmer drought severity index: Limitations and assumptions." *J. Clim. Appl. Meteorol.*, 23(7), 1100–1109.

Box, G. E. P., and Cox, D. R. (1964). "An analysis of transformations." *J. R. Stat. Soc.*, 26(2), 211–252.

Dai, A. (2011). "Characteristics and trends in various forms of the Palmer drought severity index during 1900–2008." *J. Geophys. Res.*, 116, D12115.

Dezman, L. E., Shafer, B. A., Simpson, H. D., and Danielson, J. A. (1982). "Development of a surface water supply index—A drought severity indicator for Colorado." *Int. Symp. on Hydrometeorology*, American Water Resources Association, Middleburg, VA.

Dracup, J. A., Lee, K. S., and Paulson, E. G. (1980). "On the definition of drought." *Water Resour. Res.*, 16(2), 297–302.

Dunn, R. S. (2010). "Drought." *Handbook of Texas*, Texas State Historical Association, ⟨http://www.tshaonline.org/handbook/online/articles/ybd01⟩ (Feb. 4, 2014).

Guttman, N. B., Wallis, J. R., and Hosking, J. R. M. (1992). "Spatial comparability of the Palmer drought severity index." *Water Resour. Bull.*, 28(6), 1111–1119.

Hayes, M. J., Wilhelmi, O. V., and Knutson, C. L. (2004). "Reducing drought risk: Bridging theory and practice." *Nat. Hazards Rev.*, 10.1061/(ASCE)1527-6988(2004)5:2(106), 106–113.

Hillel, D. (1982). *Introduction to soil physics*, Academic Press, New York.

IBHS (Idaho Bureau of Homeland Security). (2010). "State of Idaho hazard mitigation plan." ⟨http://www.bhs.idaho.gov/Resources/PDF/SHMPFinalw-signatures.pdf⟩ (Aug. 20, 2014).

Karl, T. R. (1983). "Some spatial characteristics of drought duration in the United States." *J. Clim. Appl. Meteorol.*, 22(8), 1356–1366.

Keyantash, J., and Dracup, J. A. (2002). "The quantification of drought: An evaluation of drought indices." *Bull. Am. Meteorol. Soc.*, 83(8), 1167–1180.

Kogan, F. N. (2000). "Contribution of remote sensing to drought early warning." *Early warning systems for drought preparedness and drought management*, D. A. Wilhite, M. V. K. Sivakumar, and D. A. Wood, eds., World Meteorological Organization, Lisbon, Portugal, 75–87.

Lloyd-Hughes, B., and Saunders, M. A. (2002). "A drought climatology for Europe." *Int. J. Climatol.*, 22(13), 1571–1592.

Manuel, J. (2008). "Drought in the southeast: Lessons for water management." *Environ. Health Perspect.*, 116(4), A168–A171.

McKee, T. B., Doesken, N. J., and Kleist, J. (1993). "The relationship of drought frequency and duration to time scales." *8th Conf. on Applied Climatology*, American Meteorological Society, Boston, 179–184.

Mishra, A. K., and Singh, V. P. (2010). "A review of drought concepts." *J. Hydrol.*, 391(1–2), 202–216.

Niemeyer, S. (2008). "New drought indices." *Options Méditerranéennes Série A: Séminaires Méditerranéens*, 80, 267–274.

Palmer, W. C. (1965). "Meteorological drought." *Research Paper No. 45*, Weather Bureau, U.S. Dept. of Commerce, Washington, DC.

Palmer, W. C. (1968). "Keeping track of crop moisture conditions, nationwide: The new crop moisture index." *Weatherwise*, 21(4), 156–161.

Paulo, A. A., Rosa, R. D., and Pereira, L. S. (2012). "Climate trends and behaviour of drought indices based on precipitation and evapotranspiration in Portugal." *Nat. Hazards Earth Syst. Sci.*, 12(5), 1481–1491.

Razali, N. M., and Wah, Y. B. (2011). "Power comparisons of Shapiro-Wilk, Kolmogorov-Smirnov, Lilliefors, and Anderson-Darling tests." *J. Stat. Model. Anal.*, 2(1), 21–33.

Ryu, J. H., Lee, J., Jeong, S., Park, S. K., and Han, K. (2011). "The impacts of climate change on local hydrology and low flow frequency in the Geum River basin, Korea." *Hydrol. Process.*, 25(22), 3437–3447.

Ryu, J. H., Palmer, R. N., Jeong, S., and Lee, J. (2004). "Drought definitions and forecasts for water resources management." *Proc., Journal of Water Resources Planning and Management, EWRI Congress 2004*, ASCE, Reston, VA.

Ryu, J. H., Sohrabi, M. M., and Acharya, A. (2014). "Toward mapping gridded drought indices to evaluate local drought in a rapidly changing global environment." *Water Resour. Manage.*, 28(11), 3859–3869.

Ryu, J. H., Svoboda, M. D., Lenters, J. D., Tadesse, T., and Knutson, C. L. (2010). "Potential extents for ENSO-driven hydrologic drought forecasts in the United States." *Clim. Change*, 101(3–4), 575–597.

Shapiro, S. S., and Wilk, M. B. (1965). "An analysis of variance test for normality (complete samples)." *Biometrika*, 52(3/4), 591–611.

Sohrabi, M. M., Ryu, J. H., Abatzoglou, J., and Tracy, J. (2013). "Climate extreme and its linkage to regional drought over Idaho, USA." *Nat. Hazards*, 65(1), 653–681.

Thornthwaite, C. W. (1948). "An approach toward a rational classification of climate." *Geog. Rev.*, 38(1), 55–94.

USGS (United States Geological Survey). (2015). "The national map viewer and download platform." ⟨http://nationalmap.gov/viewer.html⟩ (Feb. 20, 2015).

Vaezi, R. (2013). "Soil properties affecting rainfall water use efficiency (RWUE) in wheat dry-farming lands, NW Iran." *J. Agric. Sci.*, 5(6), 9–19.

Van der Schrier, G., Jones, P. D., and Briffa, K. R. (2011). "The sensitivity of the PDSI to the Thornthwaite and Penman-Monteith parameterizations for potential evapotranspiration." *J. Geophys. Res.*, 116(D3), D03106.

Veihmeyer, F. J., and Hendrickson, A. H. (1927). "Soil-moisture conditions in relation to plant growth." *Plant Physiol.*, 2(1), 71–82.

Vicente-Serano, S. M., and Lopez-Moreno, J. I. (2005). "Hydrological response to different time scales of climatological drought: An evaluation of the standardized precipitation index in a mountainous Mediterranean basin." *Hydrol. Earth Syst. Sci.*, 9(5), 523–533.

Vicente-Serrano, S. M., Begueria, S., and Lopez-Moreno, J. I. (2010). "A multiscalar drought index sensitive to global warming: The standardized precipitation evapotranspiration index." *J. Clim.*, 23(7), 1696–1718.

Wells, N., Goddard, S., and Hayes, M. J. (2004). "A self-calibrating Palmer drought severity index." *J. Clim.*, 17(12), 2335–2351.

Wilhite, D. A., and Glantz, M. H. (1985). "Understanding the drought phenomenon: The role of definition." *Water Int.*, 10(3), 111–120.

Yevdjevich, V. (1967). "An objective approach to definitions and investigations of continental hydrologic droughts." *Hydrology Papers*, Colorado State Univ., Fort Collins, CO.

Zargar, A., Sadiq, R., Naser, B., and Khan, F. I. (2011). "A review of drought indices." *Environ. Rev.*, 19, 333–349.